Low-Frequency Noise in Nonlinear Systems: Its Impact on RF Performance and Implications for Device Modeling and Circuit Simulation

Low-Frequency Noise in Nonlinear Systems

Matthias Rudolph and Fabrizio Bonani

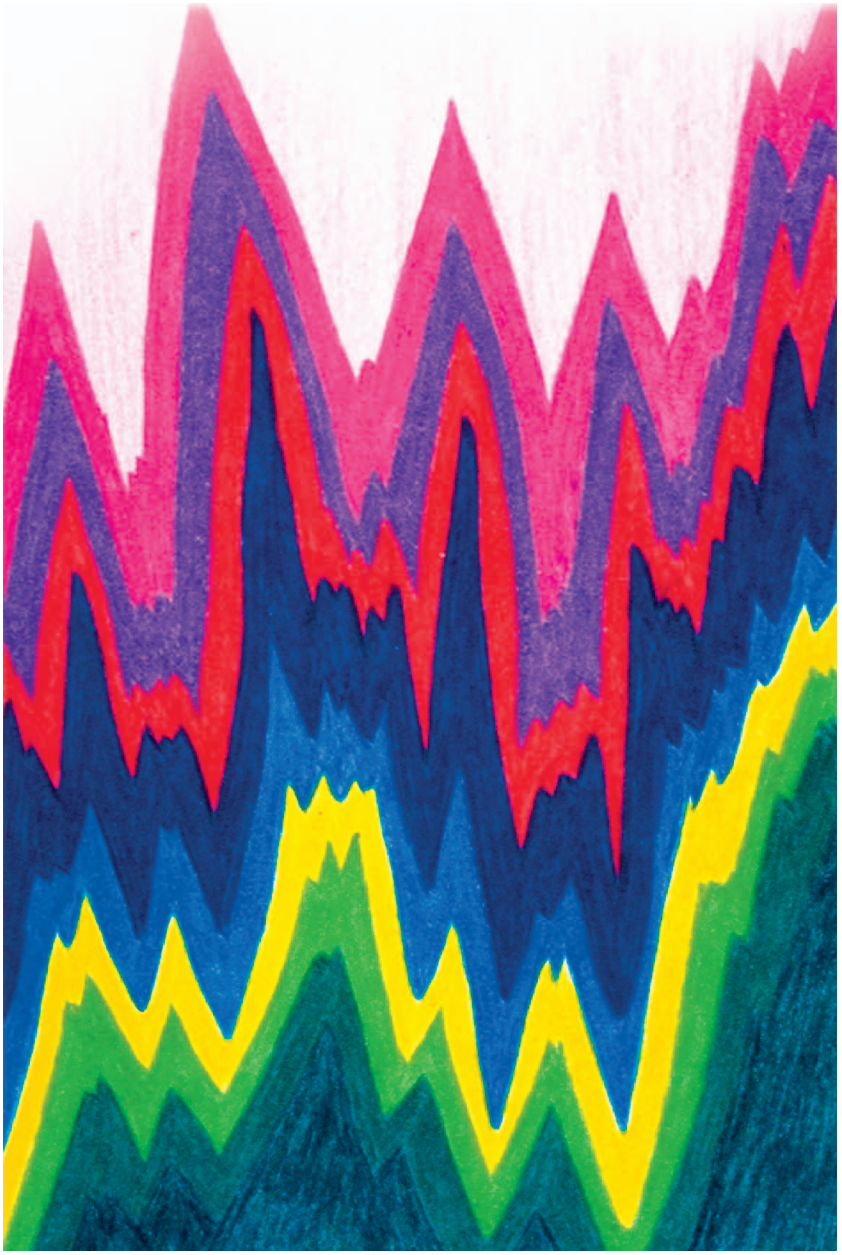

© COREL

Excess noise degrades circuit performance in linear and nonlinear operation. The linear case, obviously, is much easier to analyze, understand, and model. Things get much more involved when nonlinear operation is involved. An analytical investigation is usually not feasible, thus it is necessary to resort to numerical circuit simulation.

Furthermore, low-frequency and 1/f noise, though observed at low frequencies, also degrades RF performance whenever it is upconverted. This happens, for instance, during frequency generation in an oscillator. The upconverted low-frequency noise adds noise shoulders to the carrier, which are observed, at least for oscillators, as phase noise. But the spectral purity is also affected in mixers and amplifiers, due to the same mechanism (see Figure 1). Baseband noise is upconverted in a nonlinear circuit, which is well known from mixer theory and does not need much explanation here.

Matthias Rudolph is with Ferdinand-Braun-Institut für Höchstfrequenztechnik, Gustav-Kirchhoff-Str. 4, 12489 Berlin, Germany, E-mail: rudolph@fbh-berlin.de.
Fabrizio Bonani is with Politecnico di Torino, Dipartimento di Elettronica, Corso Duca degli Abruzzi 24, 10129 Torino, Italy, E-mail: fabrizio.bonani@polito.it.

Digital Object Identifier 10.1109/MMM.2008.930678

How the low-frequency noise processes interact with time-dependent excitation is much less clear.

In this article, we review some recent achievements regarding behavior and modeling of low-frequency noise sources that have the potential to improve phase noise simulations significantly. We start from a heuristic interpretation of how time-varying currents affect low-frequency noise sources, review physics-based device simulations, and then present how the sources can be implemented in commercial circuit simulators. Finally, simulations and measurements of GaAs-based heterojunction bipolar transistors (HBTs) are presented.

Low-Frequency Noise in a Nonlinear System

The low-frequency noise level depends on the current flowing through the device, thus qualifying it as excess noise. The common way to characterize low-frequency noise performance is to measure the baseband noise when the device is operated in different bias points. A fitting formula for an equivalent noise source, describing the noise as a function of frequency and bias can be extracted from these measurements. As an example, Figure 2 shows measured and simulated data of the low-frequency, short-circuit collector noise current of a $3 \times 30\ \mu\text{m}^2$ GaAs HBT at three different bias points. The frequency slope (near 1/f) and the characteristic corner frequency (around some 100 kHz in our case) are the same for all of the curves, while the noise level increases with collector dc current.

The model shown in the figure is described as a superposition of three noise sources: White shot noise of the base-emitter junction, a $f^{-\alpha}$ noise below some kHz, and a Lorentzian noise that is responsible for the corner frequency. The power spectral density of the last one, e.g., can be modeled as a function of base current I_b and frequency f:

$$S_{IL} = \frac{K}{1 + (f/F)^2} \cdot I_b^A, \qquad (1)$$

where K, A, and F are parameters.

What if the exciting current I_b is not constant? The first, and most common, assumption is that the dc component of the current is determining the noise. However, more detailed investigations show that this is too simplistic. Recent results suggest that at least some of the sources turn out to be driven by the instantaneous current, not only by its average value (the dc component). If the noise power level of a noise source is a function of a periodic time-varying current, one speaks of cyclostationary noise sources [1]. Cyclostationary noise sources have two important properties with regard to circuit performance (see Figure 3):

- Even if the whole circuit is perfectly linear, noise sidebands will be generated around the carrier. These are not mixing products since no nonlinearity is present, but they are generated by the time-varying, cyclostationary source itself.
- Noise sidebands will be observed in presence of an RF signal, even without a dc current, e.g., in resistive mixers.

These properties are easily derived from (1). A function of current (i.e., I_b^A) is multiplied with a function that determines the spectrum. Hence, just like in a mixer, the baseband spectrum is upconverted to the various harmonics of the current according to their magnitude.

This concept of cyclostationary noise is not easy to accept at a first glance. Since we learned that low-frequency and 1/f noise result from slow processes like generation and recombination with the associated long time constants, why should this slow process follow a fast varying signal in the microwave range?

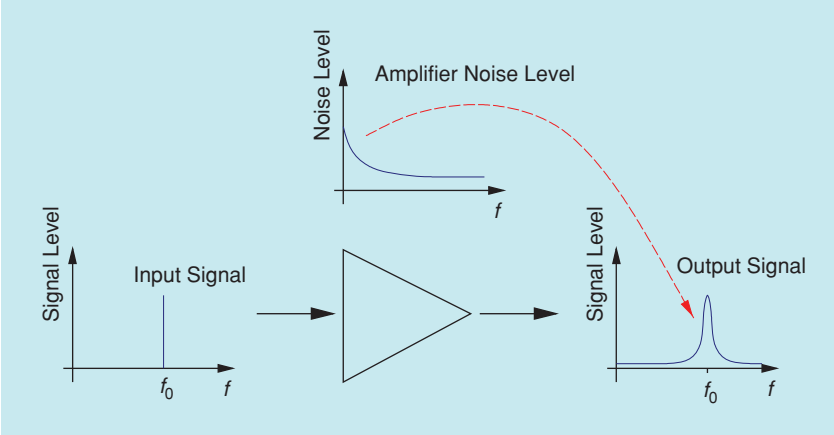

Figure 1. *Residual phase noise. If an RF signal passes through an amplifier with nonlinear or linear time-varying characteristics, the phase noise is increased due to upconversion of the amplifier low-frequency noise contribution.*

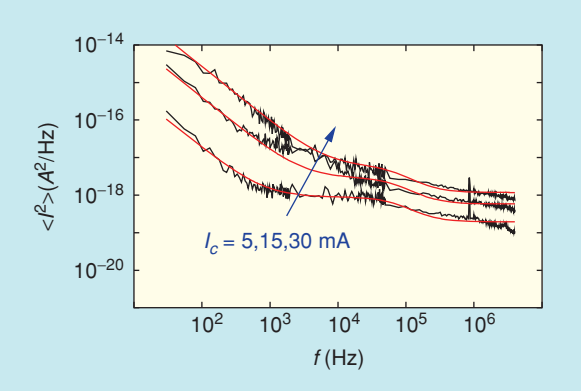

Figure 2. *Typical collector short-circuit noise-current spectrum of* $3 \times 30\ \mu\text{m}^2$ *GaAs HBT with dc collector current as a parameter.*

In the following, the properties of the low-frequency noise will be explained and simulated in the example of generation-recombination (GR) noise. Its power spectral density shows a Lorentzian frequency dependence with a characteristic time constant. Therefore, it is assumed that other spectral shapes like, e.g., 1/f, are caused by a superposition of different GR processes. Generation and recombination are not the only origin of low-frequency noise. However, as seen in compact transistor modeling, the conclusions drawn from the GR case can be generalized and provide significant improvement in circuit simulation even though the individual noise processes are not known in detail.

Slow Processes and Cyclostationary Sources

In order to explain the origin of cyclostationary noise, we will look at GR noise that can cause a Lorentzian spectrum as given in (1). Within this section, we will concentrate on how a low-frequency noise source can become cyclostationary. For a more detailed introduction to low-frequency noise in general, please refer to [2].

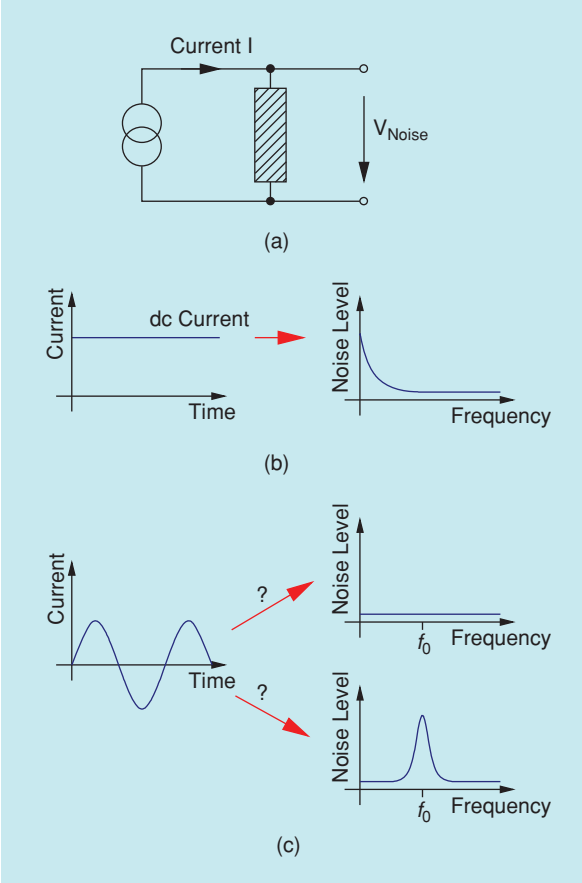

Figure 3. *Low-frequency noise of a linear resistor. (a) A current is forced through the resistor, and the noise voltage is measured, (b) low-frequency noise is observed for a dc current, and (c) if a pure RF current (without dc component) is applied. No baseband low-frequency noise is observed, but in case of a cyclostationary source, noise sidebands due to upconverted low-frequency noise are observed.*

The Shape of the Noise Spectrum

If a number of electrons is captured in a trap, the number of free carriers is perturbed. This, in turn, is observed as a current fluctuation. A trap continuously captures and releases electrons, which cause the nominally constant current to jump between two levels.

However, the impact of a single trapping or release event is not visible in time-domain measured current. Since many individual traps contribute to the noise, it looks continuous, and no discrete levels are observed.

The autocorrelation function of this perturbation will decay according to a $e^{-t/\tau}$-law, with a characteristic time constant τ (see Figure 4). This time constant corresponds to the average time for which the trap captures an electron. Each event of electron capture results in a pulse-like reduction of current with an average duration τ until the electron is released again. In the frequency domain, the time constant is also observed in the shape of the spectral power density, as it determines the corner frequency.

It is well known that a short pulse in time corresponds to a spectrum with high corner frequency, and vice versa. In our example, the spectrum given in (1) corresponds to a process that yields an autocorrelation

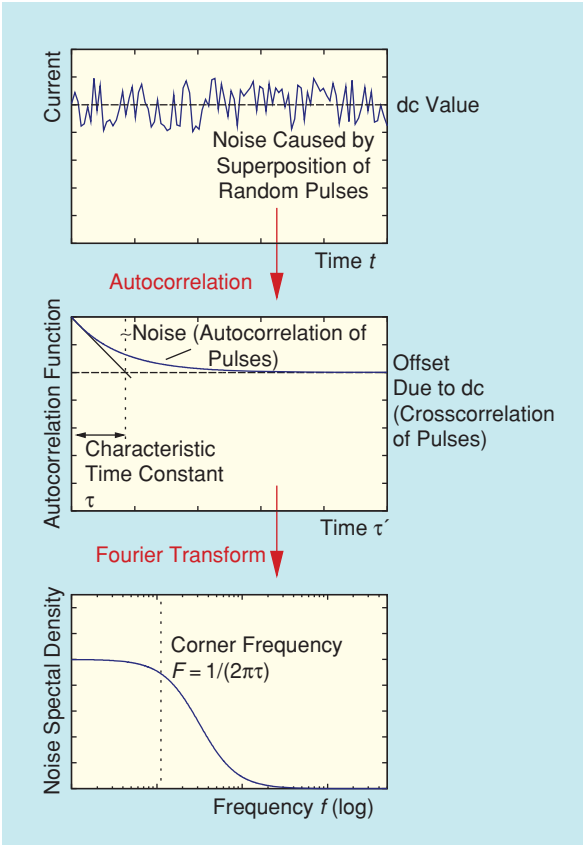

Figure 4. *If noise is caused by a random series of identical pulses, its frequency dependence is defined by the Fourier transform of the autocorrelation function of the individual pulse. Shorter pulses yield higher corner frequencies, and vice versa.*

function shaped like $e^{-t/\tau}$. With the corner frequency $F = 1/(2\pi\tau)$, it is obvious that a slower process (longer time constant τ) results in a lower corner frequency.

Average or Instantaneous Current?

So far, nothing has been said about the power level of the noise. In general, one can assume that the number of trapping events (and thus the noise power) will increase if the number of electrons (and thus the current) is increased. The measurement given in Figure 2 shows this dependence.

It is easy to accept that the noise is given by the current density if the current is either constant or varies with time constants that are large compared to the noise characteristic time-constant τ. In order to understand what happens in presence of a large-signal RF excitation, however, we need to consider the basic underlying random process.

In case of the trap-related GR noise treated in our example, it is the capture of electrons, i.e., electrons jumping from the conduction band to a trap level, which happens virtually instantaneously. Therefore, if the current changes, the number of captured electrons changes accordingly, even if the transients of the current are fast. In case of a sinusoidal current, the spectral noise power density will therefore become a periodic function in time, i.e., it becomes cyclostationary. Notice that the same discussion can be carried out for holes.

Let's summarize this statement in two steps.

1) A fraction of the electrons changes its energy level, from conduction band to trap state, randomly and instantaneously. The quantity of electrons is controlled by the instantaneous current.
2) This trapping of electrons causes a perturbation in the number of free carriers, which remain captured for a characteristic time, depending on the trap. Since this time constant is of a significant duration as compared to the microwave frequencies, low-frequency noise is observed.

While it is hard to believe at first glance that a low-frequency or 1/f noise source could become cyclostationary at all, it should be quite clear now how it does. The frequency dependence of the noise is determined by the long time constant of a secondary process that is triggered by a fast process that determines the power level.

The Noise Correlation Matrix (SCM)

For linear applications, low-frequency noise is fully characterized by its spectral density, e.g., as given by S_{IL} in (1). In the cyclostationary case, if the noise source is controlled by a current that can be described by a number of harmonics, a convenient way to describe the noise spectrum is a superposition of the noise sidebands at these harmonics. S_{IL0} refers to the baseband low-frequency noise, and $S_{IL1}, S_{IL2}, \ldots S_{ILn}$ describe the noise sidebands at first, second, and nth harmonic. Since these noise sidebands are the result of a memoryless mixing process, all have the same frequency shape (although shifted in frequency towards the corresponding harmonic) but with different magnitude.

Noise measured at different frequencies is uncorrelated in the linear case. This no longer holds true if a noise spectrum results from a mixing process, as in the case of a cyclostationary source. The upconversion establishes a relation between the noise at a baseband frequency f_x and the noise at the corresponding frequencies resulting from a mixing process at $f = f_n \pm f_x$, with f_n being the nth harmonic. In order to fully characterize a cyclostationary source, this interfrequency crosscorrelation also has to be quantified. This information can be written in the form of an interfrequency noise correlation matrix [also called *sideband correlation matrix (SCM)*]

$$C_{IL} = \begin{pmatrix} S_{IL0} & S^*_{IL10} & \cdots & S^*_{ILn0} \\ S_{IL10} & S_{IL1} & \cdots & S^*_{ILn1} \\ \vdots & \vdots & \ddots & \vdots \\ S_{ILn0} & S_{ILn1} & \cdots & S_{ILn} \end{pmatrix}. \qquad (2)$$

Notice that the SCM, despite being similar to the standard (stationary) noise correlation matrix because the diagonal elements define the autocorrelation spectra, is actually deeply different. In fact, in the linear case, each diagonal element represents the noise power spectrum at a specific device port. Each diagonal element of the SCM, on the other hand, represents the noise power around each of the harmonics of the same port, while off-diagonal terms represent the correlation between the corresponding noise sidebands. In other words, the SCM has some similarity with the conversion matrix well known from mixer theory.

A System Oriented Interpretation

From a system-oriented point of view, generation of low-frequency noise can be described in two different ways, as shown in Figure 5. Both setups consist of the same elements. In both cases, we start with a white noise process that yields a constant (as a function of frequency and of the bias point) average, normalized noise power. In the classical low-pass case, this white noise is weighted by a function of current, which determines the power level, and afterwards low-pass filtered. The transfer function of the filter is chosen according to the frequency dependence of the noise to be modeled. As a result, the final low-pass filtering ensures that only baseband noise is observed.

If the mixing process and the filtering are exchanged, nothing happens in the dc range. But if the current is time variant, the baseband noise is multiplied by all the harmonics of the current and therefore upconverted, yielding noise sidebands at all harmonic frequencies in addition to baseband noise. Hence, this implementation yields cyclostationary noise.

What remains is the question on which of these two compact representations yields better results when compared to real devices. This will be discussed in the following sections.

Some Important Results from Physical Device Simulation

In this section, results from physical simulation will be reviewed that highlight the link between the microscopic cyclostationary noise sources within the device and the noise measured at the device terminals. Unlike a measurement, this simulation allows control of the internal physical properties and, therefore, provides the possibility of understanding the impact of the cyclostationarity of the individual distributed microscopic sources on port noise currents of the lumped element.

The two system-oriented approaches discussed in the previous section can be applied to more general colored or white noise processes [9], [10]: in the latter case, they obviously give rise to the same result (in fact, the filtering stage is simply absent). This suggests a possible use of physics-based device noise simulation to help in choosing between the low-pass and cyclostationary approaches. In fact, in many important cases, low-frequency noise is obtained as a superposition of Lorentzian spectra resulting from noninteracting traps. Also, trap-assisted GR noise can be simulated in physical models, making use of white microscopic noise sources [8] (this is the physical counterpart of the heuristic discussion above), thereby avoiding any ambiguity in the modulation taking place in case of upconversion. For a detailed description of the physical model, see [8].

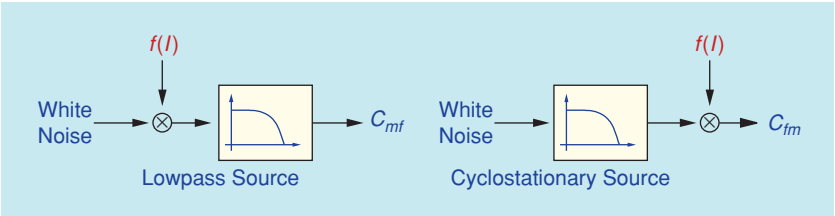

Figure 5. *System-oriented description of the low-frequency noise in nonlinear operation.*

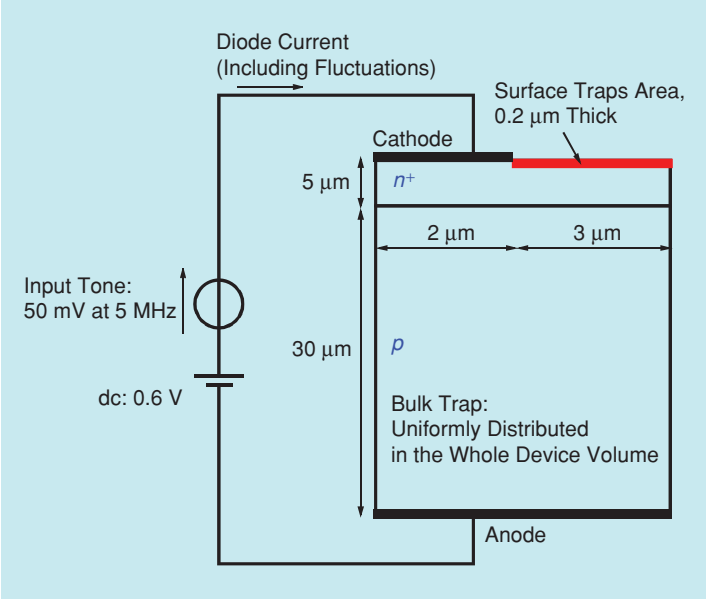

Figure 6. *Schematic representation of the two-dimensional diode structure for physics-based simulations.*

This pattern has been followed in [11], where a *pn* diode with four trap levels has been simulated when operated in large-signal conditions due to a voltage input tone applied to the device. One trap is uniformly distributed within the device volume (bulk trap), while the other three are concentrated into a thin slice of semiconductor (in the neutral, resistive region of the device) to simulate low-frequency noise due to surface traps (see Figure 6).

The parameters of the three surface traps (see [11] for details) are chosen to yield a $1/f$ contribution to the terminal current noise in small-signal operation, while the bulk trap results in a low-pass behavior. This is confirmed by Figure 7, where the four contributions to the stationary (i.e., small-signal) GR noise current spectrum (the various traps are considered to be noninteracting) are plotted for a dc bias of 0.6 V.

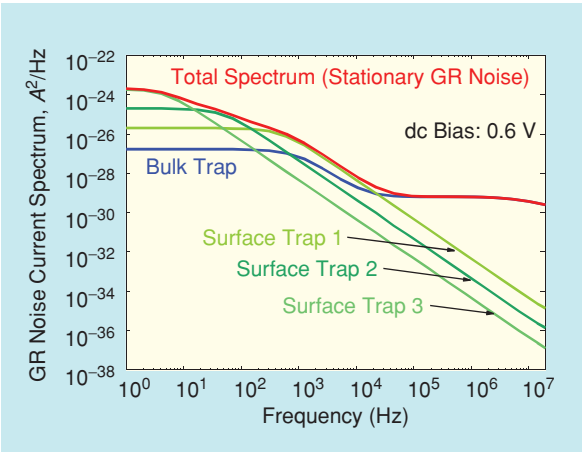

Figure 7. *Simulated stationary current noise spectra due to GR processes in the four traps.*

Large-signal, nonlinear operation is simulated by adding a 50 mV input tone at the frequency of 5 MHz to the 0.6 V dc bias, thus providing a significant generation of harmonics in the device. (More details on the simulation parameters can be found in [11].) The most interesting result is obtained by checking the element of the noise correlation matrix (SCM) corresponding to the first harmonic, since this spectrum should contain also the upconverted low-frequency noise contribution. In

Figure 8, the (+1, +1) element of the noise correlation matrix is reported as a function of the offset frequency from the first harmonic, which corresponds to the noise sideband of the fundamental frequency. It is observed that the noise generated by the bulk trap is much stronger converted to upper sidebands than the surface traps, basically because the bulk trap noise is mainly generated in the diode depletion region, i.e., a strongly nonlinear device area. Surface traps, on the other hand, are placed in a resistive region, whose nonlinearity is much milder.

This physical device simulation yields the unexpected result that even though all distributed microscopic noise sources indeed show cyclostationary behavior, this property may not be observed in every case if the noise is to be described by the port noise quantities (i.e., a lumped current sources controlled by the total port current). Hence, this result is the physical foundation for the use of both low-pass and cyclostationary noise sources discussed in the following section.

Defining Cyclostationary Sources for Compact Transistor Models

Microwave circuits are traditionally simulated in the frequency domain with harmonic balance simulators. These represent voltages and currents in the frequency domain and thus are well suited for circuits like mixers or oscillators, where the signals can be characterized by a few harmonics. In addition, passive elements can be easily defined in the frequency domain, which also facilitates the implementation of dispersive effects and distributed structures. Commercial harmonic balance simulators currently do not provide built-in cyclostationary noise sources. It is possible to define a low-frequency noise source with different frequency dependencies, e.g., as defined in (1), which will be used as an example. However, only the dc component of the exciting current is considered when the noise is calculated. It is therefore necessary to force the simulator to use the instantaneous current; this is easily achieved using the subcircuit shown in Figure 9 [3]. The main idea is to split (1) into two parts. The first one describes the frequency dependence of the low-frequency noise, implemented as a normalized noise source given by

$$\left\langle |i'|^2 \right\rangle = \frac{K}{1 + (f/F)^2}. \tag{3}$$

In order to ensure that the noise source is driven by the instantaneous current is Ib, it is used to drive a controlled current source

$$i'' = \sqrt{I_b^A}. \tag{4}$$

The instantaneous current is a time domain quantity, in contrast to the noise that is defined in frequency domain. The task to combine these two to get a time-domain current fluctuation, or a noise spectrum, is basically the task of the simulator. In the model, both quantities are measured by feeding the currents through 1 Ω resistors. In order to produce a noise source as defined in (1), the currents provided by (3) and (4) are multiplied. In the equivalent circuit, a controlled current source is used, providing the two nodes of the cyclostationary noise source. The multiplication takes place in the time domain. In the frequency domain, it results in the upconversion of the baseband noise defined in (3), which yields noise sidebands at the harmonics of the driving current. The current source is defined by

$$i'''(t) = v_a(t) \cdot v_b(t) \cdot (A^2/V^2). \tag{5}$$

This implementation is quite straightforward and yields a noise source that presents noise sidebands at all harmonics. However, simply mixing low-frequency noise with the current results in strong correlation of the noise sidebands. While this simple implementation works well in many cases, it may be necessary to control the correlation sometimes.

A possible subcircuit is shown in Figure 10. It allows decoupling of the harmonic noise sidebands from the baseband noise. An *RC* circuit is used to distinguish between the dc and RF part of the controlling instantaneous current. The required voltage source provides a

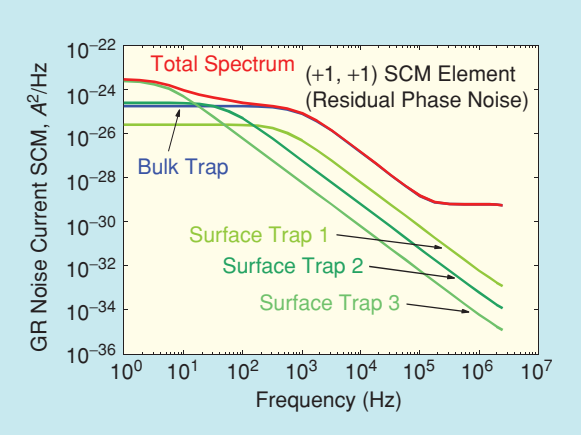

Figure 8. *Simulated cyclostationary current noise spectra due to GR processes in the four traps. Only the (+1, +1) element of the SCM (corresponding to the noise at the fundamental frequency) is depicted.*

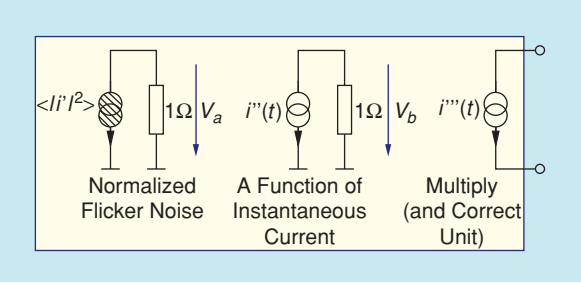

Figure 9. *Subcircuit that realizes cyclostationary noise source in HB simulators.*

voltage of the same magnitude as the current source (4). The value of the capacitance is chosen to achieve a corner frequency well below the first harmonic of the signal.

Three low-frequency noise sources are required. Two of them, $\langle|i'_1|^2\rangle$ and $\langle|i'_2|^2\rangle$, will be used to define the uncorrelated parts of RF and baseband noise, the third one, $\langle|i'_3|^2\rangle$, will be present at all frequencies in order to realize the correlated part of the noise. A correlation factor $0 < F_c < 1$ controls the correlation. The three sources read as follows:

$$\langle|i'_1|^2\rangle = (1 - F_c) \cdot \frac{K}{1 + (f/F)^2} \quad \text{(baseband noise)} \quad (6)$$

$$\langle|i'_2|^2\rangle = (1 - F_c) \cdot \frac{K}{1 + (f/F)^2} \quad \text{(RF noise)} \quad (7)$$

$$\langle|i'_3|^2\rangle = F_c \cdot \frac{K}{1 + (f/F)^2} \quad \text{(correlated part).} \quad (8)$$

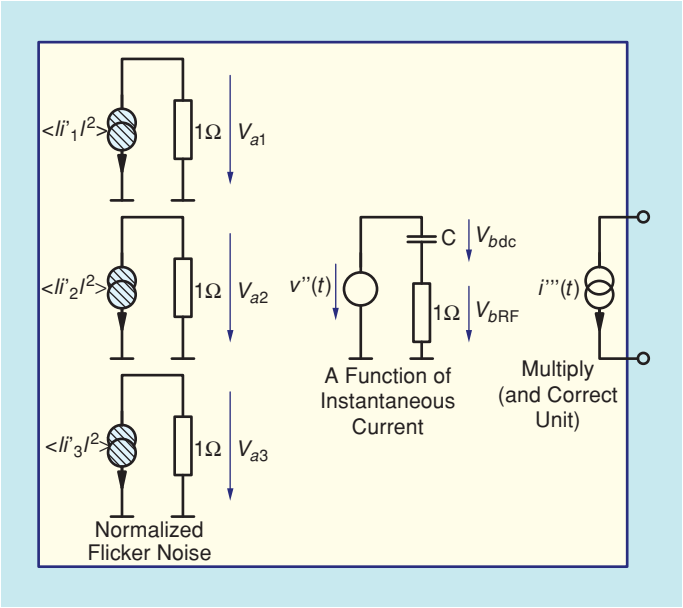

Figure 10. *Subcircuit of cyclostationary noise source that allows to control the interfrequency noise correlation.*

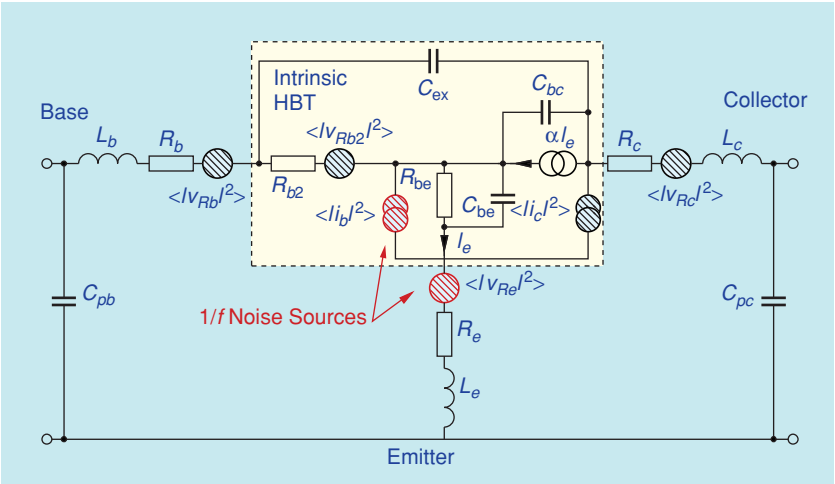

Figure 11. *Small-signal equivalent circuit of the HBT.*

Finally, the partly correlated cyclostationarity is obtained through the controlled source $i'''(t)$

$$i'''(t) = \{[v_{a1}(t) + v_{a3}(t)] \cdot v_{bDC}(t) + [v_{a2}(t) + v_{a3}(t)] \cdot v_{bRF}(t)\} \cdot (A^2/V^2). \quad (9)$$

Simulating Phase Noise of GaAs HBTs

In this section, we show to which extent the simulation accuracy can be improved when cyclostationary noise sources replace the common low-pass noise sources [5]. As an example, residual phase noise measurements of GaAs HBTs are compared with measurements.

Residual phase noise denotes the excess phase variations that arise when an RF signal passes through an amplifier. They show up as noise sidebands. In our case, the HBT is operated in class-A, and signals at comparatively low frequency (3.5 GHz, while the transition frequency is around 35 GHz) and low signal power is applied. The HBT is driven in a weakly nonlinear regime, and the frequency is low enough to ensure that no high-frequency effect gives rise to a reduction of model accuracy. The measurement is carried out in a 50-Ω environment. What is measured at the end is the excess noise near the 3.5 GHz carrier that was generated by the HBT [7], thus requiring to characterize the transistor in open-loop conditions, i.e., avoiding to measure a working oscillator. In contrast to an oscillator measurement, one can therefore freely choose bias point, frequency, and input power level of the transistor.

The HBT under test is an InGaP/GaAs HBT with an emitter area of $3 \times 30\ \mu m^2$, fabricated on the 4-in process line of the Ferdinand-Braun-Institut, Berlin, Germany. It is biased at $V_{CE} = 3$ V and $I_C = 30$ mA, $f = 3.5$ GHz.

The simulation is carried out using a commercial harmonic-balance simulator, ADS by Agilent Technologies. The model is the FBH HBT model, a dedicated GaAs HBT model. It is implemented into the ADS software using the proprietary user-complied model (UCM) C-Code interface and using the Verilog-A interface. Both implementations yield identical results. Four types of low-frequency noise implementations are compared:

1) traditional low-pass sources
2) cyclostationary sources according to Figure 9
3) partly correlated cyclostationary sources according to Figure 10
4) a superposition of cyclostationary and low-pass sources.

Figure 11 shows the corresponding small-signal equivalent circuit with noise sources. As pointed out in the literature, two low-frequency noise sources are required to fully describe the 1/f noise of the HBT. Only one source is commonly included in standard bipolar models, but it has been shown that such a model is not capable of describing the impact of a variation of the source resistance (i.e., the termination of the base-emitter port) on 1/f noise. On the other hand, it is not feasible to account for more than two sources—more sources cannot be extracted unambiguously. In our case, we attribute one low-frequency noise source to the base-emitter junction and the second one to the emitter ballasting resistor. This is a choice that can be motivated from physics, but other configurations are possible, too. In any case, it is necessary to keep in mind that this is a global integral description of the noise. It is not possible to trace back reliably to individual low-frequency noise processes located in some region of the HBT.

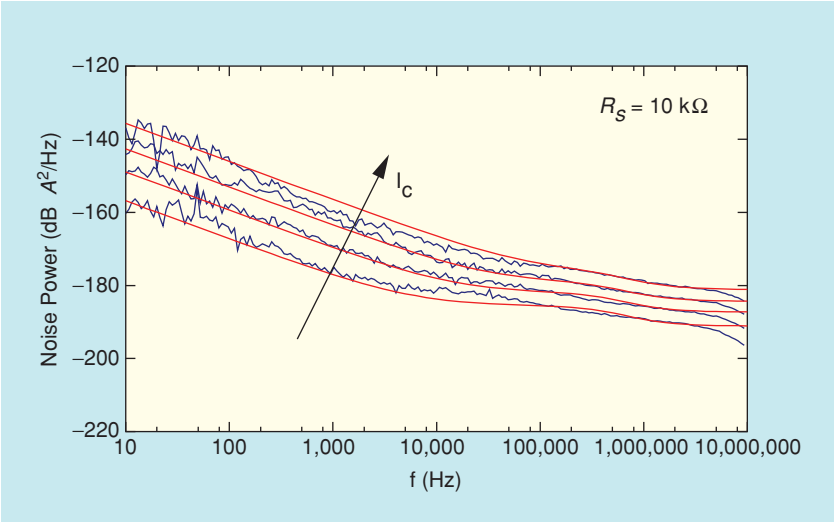

Figure 12. *Measured (blue) and simulated (red) short-circuit low-frequency noise collector current of* $3 \times 30\ \mu m^2$ *HBT at* $V_{CE} = 3$ V, $I_c = 2.5, 5, 10, 20$ mA.

After the large-signal parameters have been determined, the low-frequency noise is measured at different source resistances to extract the respective parameters. Figure 12 shows measurements and simulations for different collector currents for the high-impedance case. The agreement is very good for all four models, since they indeed are identical in the linear case.

Figure 13 presents measurement and simulation of residual phase noise at 3.5 GHz. Regarding the measurement at an available input power $P_{in} = -11$ dBm [Figure 13(a)] it is obvious that the standard low-pass source implementation (blue line) does not yield acceptable accuracy. If cyclostationary sources (red lines) are considered, on the other hand, close agreement between measurement and simulation is observed. This type of implementation also has been shown to yield accurate simulations of oscillator phase noise [4], [6].

In rare occasions, however, the cyclostationary approach fails, as can be seen in Figure 13(b) below $\Delta f = 100$ Hz (red curve). The strange shape of the curve can be explained by a dispersion of the source resistance in this region: a large capacitor in

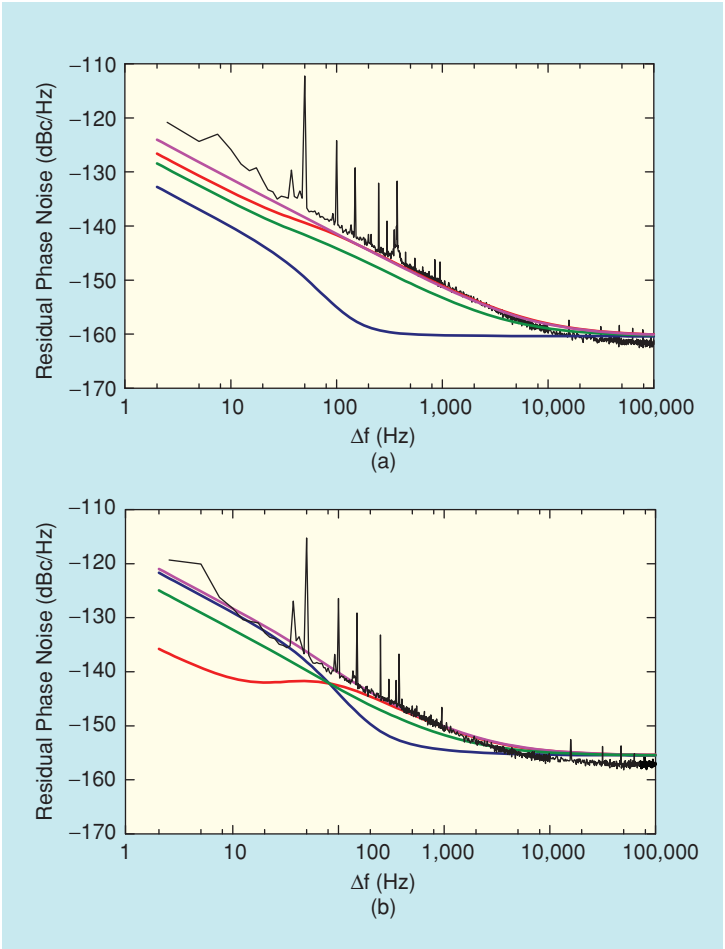

Figure 13. *Measured and simulated residual phase noise of* $3 \times 30\ \mu m^2$ *HBT with available input power (a)* $P_{in} = -11$ *dBm and (b)* $P_{in} = -16$ *dBm.* $V_{ce} = 3$ *V,* $I_c = 30$ mA, $f = 3.5$ GHz. *Measurement (black curves) compared to simulations using conventional lowpass low-frequency noise sources (blue), cyclostationary sources (red), partly correlated cyclostationary sources (magenta), and superposition of cyclostationary and lowpass sources (green).*

the measurement setup causes low source resistance for higher frequencies, while the constant-current bias presents a high resistance for lower frequencies. Either way, an operating condition is found where the cyclostationary approach clearly fails, and it is interesting to note that the low-pass sources yield a perfect fit in this region.

The only reason that the implementation based on cyclostationary noise sources yields significantly lower phase noise compared to the low-pass sources is that the noise sidebands around 3.5 GHz (from the noise source itself) and the upconverted baseband noise (due to device nonlinearity) cancel each other out. Reduction of interfrequency correlation solves the issue: the magenta curves in Figure 13 were obtained from simulations relying on partly correlated cyclostationary noise sources, with a correlation coefficient of $F_c = 0.25$.

One might argue that, instead of introducing partly correlated sources, a superposition of low-pass and cyclostationary sources should be applicable, as in the case of the physical simulations presented previously. This might also somehow reflect that different processes contribute to the two lumped noise sources. This has been tested, and the low-frequency noise sources were realized by parallel low-pass as well as cyclostationary sources. The result is shown as green lines in Figure 13. This implementation yields the correct shape of the measured residual phase noise, but the results are always 3 dB below those of the partially correlated noise source approach. This finding is not surprising since only 50% of the total power level is available in the relevant part of the source (low-pass or cyclostationary). However: regarding all factors in a phase noise simulation, a 3 dB offset is not so far away from the ideal result, and the shape of the simulated curves is described correctly. Also, the mixed low-pass-cyclostationary approach looks feasible for circuit design.

Conclusion

Low-frequency noise can be driven by the instantaneous current, e.g., if it is caused by GR processes. In the case of nonlinear operation, this means that it does not only show up at baseband, but also is observed as noise sidebands at the large-signal harmonics. It is necessary to take this property into account when simulating nonlinear circuits.

Although the microscopic noise sources might be cyclostationary, this does not necessarily hold true for the lumped sources in a compact model. The sources can show up providing pure baseband noise, they can turn out to be cyclostationary, or a mixture of both. Also, the interfrequency correlation could be lower than expected in case of cyclostationary sources. When a noise model is derived, it should be investigated by nonlinear measurement how the lumped sources are best implemented.

Even though cyclostationarity means that the noise source is excited by a time-varying current, this type of noise source is easily formulated in a way that allows using it in harmonic balance simulation. This can be achieved by representing each source by a small subcircuit. The better understanding of the nonlinear behavior of low-frequency noise sources enables significant improvement of phase-noise simulations in harmonic balance simulators.

Acknowledgments

F. Bonani acknowledges the long standing collaboration with S. Donati Guerrieri and G. Ghione of Politecnico di Torino, who are equally responsible for the understanding of low-frequency noise conversion phenomena through physical models as described in this article. He also thanks F. Bertazzi and G. Conte (Dipartimento di Elettronica, Politecnico di Torino) for setting up the simulation code and actually performing the GR noise simulations, respectively.

M. Rudolph would like to thank O. Llopis and S. Gribaldo, LAAS CNRS, Toulouse, France, for performing the residual phase noise measurements.

References

[1] T.H. Lee and A. Hajimiri, "Oscillator phase noise: A tutorial," *IEEE J. Solid-State Circuits*, vol. 35, pp. 326–336, Mar. 2000.

[2] M. Sandén and M.J. Deen, "Low-frequency noise in advanced Si-based bipolar transistors and circuits," in *Noise and Fluctuations Control in Electronic Devices*, A.A. Balandin, Ed. Valencia, CA: American Scientific Publishers, 2002, pp. 235–247.

[3] M. Margraf and G. Böck, "Analysis and modeling of low-frequency noise in resistive FET mixers," *IEEE Trans. Microwave Theory Tech.*, vol. 52, no. 7, pp. 1709–1718, July 2004.

[4] J.-C. Nallatamby, M. Prigent, M. Camiade, A. Sion, C. Gourdon, and J.J. Obregon, "An advanced low-frequency noise model of GaInP/GaAs HBT for accurate prediction of phase noise in oscillators," *IEEE Trans. Microwave Theory Tech.*, vol. 53, no. 5, pp. 1601–1612, May 2005.

[5] M. Rudolph, F. Lenk, O. Llopis, and W. Heinrich, "On the simulation of low-frequency noise upconversion in InGaP/GaAs HBTs," *IEEE Trans. Microwave Theory Tech.*, vol. 54, pp. 2954–2961, July 2006.

[6] P.A. Traverso, C. Florian, M. Borgarino, and F. Filicori, "An empirical bipolar device nonlinear noise modeling approach for large-signal microwave circuit analysis," *IEEE Trans. Microwave Theory Tech.*, vol. 54, pp. 4341–4352, Dec. 2006.

[7] G. Cibiel, L. Escotte, and O. Llopis, "A study of the correlation between high-frequency noise and phase noise in low-noise silicon-based transistors," *IEEE Trans. Microwave Theory Tech.*, vol. 52, no. 1, pp. 183–190, Jan. 2004.

[8] F. Bonani, G. Ghione, *Noise in Semiconductor Devices*. Heidelberg: Springer Verlag, 2001.

[9] A. Demir and A. Sangiovanni-Vincentelli, *Analysis and Simulation of Noise in Nonlinear Electronic Circuits and Systems*. Norwell, MA: Kluwer, 1998.

[10] F. Bonani, S. Donati Guerrieri, and G. Ghione, "Physics-based simulation techniques for small- and large-signal device noise analysis in RF applications," *IEEE Trans. Electron. Devices*, vol. 50, no. 3, pp. 633–644, Mar. 2003.

[11] F. Bonani, F. Bertazzi, G. Conte, S. Donati Guerrieri, and G. Ghione, "Key issues in trap-assisted low-frequency device noise simulation in nonlinear large-signal conditions," in *Proc. 4th Int. Conf. Unsolved Problems of Noise*, Gallipoli, Italy, June 2005, pp. 449–454.